

THE BEHAVIOR OF PCM/PM RECEIVERS IN NON-IDEAL CHANNELS

Part I: The Separate Effects of Imperfect Data Streams and Band-limiting Channels on Performance¹

Tien Manh Nguyen
National Aeronautics and Space Administration
Jet Propulsion Laboratory
California Institute of Technology
4800 Oak Grove Drive
Pasadena, CA 91109

ABSTRACT

The performance of residual carrier communication systems that are used for space telemetry signals and that employ a PCM/PM modulation technique with an imperfect NRZ or Bi- ϕ data format and band-limited channels is investigated in this paper. In this particular modulation scheme, the data (either Non-Return-to-Zero, NRZ, or Bi- ϕ) is directly modulated on the RF residual carrier. Undesired spectral components caused by the imperfect data stream (e.g., data asymmetry due to rising and falling voltage transitions or an imbalance between +1's and -1's in the data stream) can degrade the carrier tracking and symbol synchronization performances. Only the effects of imperfect carrier tracking due to an imperfect data stream are considered. The Symbol Error Rate (SER) performance degradation due to the presence of an imperfect data stream is evaluated for both NRZ and Bi- ϕ data formats, and these evaluations are compared. Furthermore, the SER performance for both PCM/PM/NRZ and PCM/PM/Bi- ϕ is analyzed for the presence of a band-limited channel. The effects of the InterSymbol Interference (ISI) created by a band-limited channel on system performance are evaluated for an ideal low-pass filter.

¹. The work described in this paper was carried out at the Jet Propulsion Laboratory, California Institute of Technology, under contract with the National Aeronautics and Space Administration,

1. Introduction

There are considerable interests among international space agencies to search for a bandwidth-efficient modulation scheme that can be used for future space missions without major modifications to their ground stations. The Consultative Committee for Space Data Systems (CCSDS) (established by nine international space agencies and eight observer agencies [1]) has undertaken the task to investigate a modulation scheme that offers both of these features (bandwidth efficiency and no major hardware modifications to the current systems.)

Currently, the space telemetry systems employ residual carrier modulation with the subcarriers which are used to separate the data from the RF residual carrier [1]. The CCSDS has recommended that squarewaves and sinewaves are used for the deep space and near earth missions, respectively. This modulation scheme is called PCM/PSK/PM and it was developed at a time when weak signals and low data rates dominated [2]. As the technology in antenna, transmitters and signal processing improved, a significant increase in the available signal power can provide much higher telemetry bit rate. For high telemetry bit rate, the use of the subcarrier causes the occupied bandwidth to increase significantly [3]. This is prohibitive because the space telemetry systems often operate under imposed bandwidth constraints. A natural solution is to use the residual carrier modulation without the subcarriers. This modulation scheme is referred to as PCM/PM. Because this modulation technique requires a minimum hardware modification to the current systems and, at the same time, the bandwidth efficiency can be achieved. Recently, [4] has compared the performance of PCM/PM and PCM/PSK/PM modulation techniques for space telemetry applications. The results presented in [4] show that, for certain operating conditions, the performance of PCM/PM/NRZ will be as good as PCM/PM/Bi- ϕ or PCM/PSK/PM. Furthermore, [5] also shows that PCM/PM/NRZ provides smaller occupied bandwidth as compared to PCM/PSK/PM and PCM/PM/Bi- ϕ . However, the results shown in [4-5] were derived based on perfect operating conditions, e.g., perfect data stream with balanced +1's and -1's and unlimited bandwidth channel.

In the recent past, [6-8] have investigated only the effects of data asymmetry and bandlimiting channel on the performance of space telemetry systems. However, [6] only considers the effects of NRZ data asymmetry on PCM/PSK/PM systems with squarewave subcarriers, and [7] only investigates the effects of data asymmetry of a perfectly balanced Bi- ϕ data stream on the carrier tracking performance and the consequent effect upon the probability of error. On the other hand, [7] only analyzes the effects of data asymmetry and bandlimiting channel on the performance of suppressed carrier systems. Furthermore, when analyzing the effects of bandlimiting, [7] has assumed that (1) the amount of data asymmetry is known so that an optimum sampling time can be set for the sample detector, and (2) the carrier tracking is perfect.

The goal of this paper is to investigate and assess the impacts of imperfect data stream and bandlimiting channel conditions on the performance degradation of the space telemetry receivers in the presence of the PCM/PM signals. Separate effects of data asymmetry, unbalanced data stream and ISI caused by band-limited channel on

performances of PCM/PM/NRZ and PCM/PM/Bi- ϕ receivers are analyzed. This extends previously reported work that assumed ideal operating conditions [4-8].

This paper is organized in the following manner. Section 2 introduces the space telemetry system models employing PCM/PM modulation technique. Section 3 investigates the effects of data asymmetry on the system performance. The effects of imbalance between +1's and -1's in the data streams are analyzed in Section 4. Section 5 presents the analysis for band-limited channel. Numerical results and discussions are shown in Section 6. Finally, Section 7 presents the main conclusion of the paper.

2. Space Telemetry System Models

Figure 1 illustrates a space telemetry system model in which the data stream can be either NRZ or Bi- ϕ (Bi-phase or Manchester) data stream with a transition density, p , which is less than or equal to 1/2. In this model the transmitted telemetry, signal is given by

$$S_t(t) = \sqrt{2P} \cos(\omega_c t + \text{mid}(t)) \quad (1)$$

where P is the transmitted power, $\omega_c = 2\pi f_c$ is the angular carrier center frequency in rad/sec, m_T is the telemetry modulation index in rads which is less than $\pi/2$, and $d(t)$ is NRZ data Sequence (PCM/PM/NRZ) or the Manchester data waveform generated by the binary (± 1) NRZ data sequence (PCM/PM/Bi- ϕ). Figures 2(a) and 2(b) show the plots of the power spectral densities of $S_t(t)$ for PCM/PM/Bi- ϕ and PCM/PM/NRZ, respectively.

The received signal $S_r(t)$ is corrupted by additive white Gaussian noise $n(t)$ with one-sided noise spectral density N_0 and data asymmetry or unbalanced data stream. Expanding the received signal we have

$$S_r(t) = \sqrt{2P} \left[\cos(m_T) \cos(\omega_c t + \theta_o) - d(t) \sin(m_T) \sin(\omega_c t + \theta_o) \right] + n(t) \quad (2)$$

where ω_o is the initial phase offset caused by the transmission medium. The first and second terms of Eqn (2) are the residual carrier and data components, respectively.

The data asymmetry and/or the imbalance between +1's and -1's in the data stream will produce undesired spectral components at the carrier frequency creating an imperfect carrier reference that will degrade the telemetry system performance. In addition, the ISI created by the band-limited channel can cause further disturbance to the carrier reference.

If we let $\hat{\theta}$ denote the carrier loop estimate of θ_o , the phase error θ_e due to the thermal noise and the interference caused by the data asymmetry/or unbalanced data stream is defined as

$$\theta_e = \theta_o - \hat{\theta} \quad (3)$$

The carrier loop tracks the residual carrier component in Eqn (2) to provide an imperfect reference for the modulation given by

$$r(t) = \sqrt{2} \cos(\omega_c t + \theta) \quad (4)$$

Assuming the symbol sync clock $C(t)$ as shown in Figures 3(a) and 3(b) for NRZ and $\text{Bi-}\phi$ respectively, and using the imperfect carrier reference in (4), one can show that the signal output of the integrate-and-dump at time $t = T_s$ is given by

$$Z(T_s) = \sqrt{P} \sin(m_T) \cos(\theta_e) \int_0^{T_s} d(t) C(t) dt + n(T_s) \quad (5)$$

Here one has assumed that the phase error process θ_e of Eqn (3) is essentially constant during the symbol interval T_s , and that the corrupting noise process $n(T_s)$ is a zero-mean Gaussian random variable with a variance $N_0 T_s / 2$.

The test statistic $Z(T_s)$ of Eqn (5) represents the observed data at the receiver. This test statistic is needed to determine the SER performance. Using this test statistic, the performance of the telemetry system shown in Figure 1 has been evaluated in [4] for both NRZ and $\text{Bi-}\phi$ data formats. The results of [4] are presented here for the sake of completeness. The average probability of error is given by

$$P_e = \int_{\theta_e} P_e(\theta_e) P(\theta_e) d\theta_e \quad (6)$$

where $P_e(\theta_e)$ is the conditional probability of error and $P(\theta_e)$ is the probability density function (pdf) for θ_e . For perfect data stream and ideal channel, this conditional probability of error is:

$$P_e(\theta_e) = (1/2) \operatorname{erfc}\{\sqrt{E_s/N_0} \cos(\theta_e)\} \quad (7)$$

where E_s denotes the symbol energy, i.e., $E_s = (P T_s) \sin^2(m_T)$. In this paper, one postulates a Tikhonov pdf for θ_e , which is entirely characterized by the variance σ^2 of the carrier tracking phase error. When the loop signal-to-noise ratio is high the Tikhonov pdf can be approximated by

$$P(\theta_e) \approx \exp(-\theta_e^2/2\sigma^2) / [2\pi\sigma^2]^{1/2}, \quad -\infty < \theta_e < \infty \quad (8)$$

For perfect data streams and high-data-rate case ($B_L/R_s \ll 0.1$, where B_L and R_s denote the one-sided loop bandwidth and the symbol rate, respectively), the variance of the carrier tracking phase error has been found in [4]. For perfect NRZ data format, it is found to be

$$\sigma^2 = (1/p_0) + (B_L/R_s) \tan^2(m_T) \quad (9)$$

and, for perfect Bi- ϕ data format σ^2 becomes

$$\sigma^2 = (1/\rho_0) + (I/C) \tan^2(m_T) \quad (10)$$

where

$$\rho_0 = \frac{(E_s/N_0)}{(B_1/R_s) \tan^2(m_T)}, \quad (11)$$

$$\begin{aligned} I/C = & (1/2) - t (9/16) (B_1/R_s)^{-1} \\ & - (3/4) (B_1/R_s)^{-1} \exp\{-(2/3)(B_1/R_s)\} [\cos\{(2/3)(B_1/R_s)\} + 3\sin\{(2/3)(B_1/R_s)\}] \\ & + (3/16) (B_1/R_s)^{-1} \exp\{-(4/3)(B_1/R_s)\} [\cos\{(4/3)(B_1/R_s)\} + 3\sin\{(4/3)(B_1/R_s)\}] \end{aligned} \quad (12)$$

In the following sections, one will determine the conditional error probability and the carrier tracking phase error when the data stream is disturbed by the data asymmetry or when there exists an unbalanced between +1's and -1's in the transmitting data stream. Moreover, the effects of a band-limited channel on the performance of the PCM/PM receivers are also investigated.

3. The Effects of Data Asymmetry

The telemetry data asymmetry due to rising and falling voltage transitions can cause undesired spectral components at the output of the spacecraft's transmitter. The effects of these spectral components on the performance degradation of the space telemetry receivers have been investigated in [6, 8]. As mentioned earlier, [6] and [8] investigate the PCM/PSK/PM with squarewave subcarriers and PCM/PM/Bi- ϕ modulation systems with balanced data streams, respectively. Whenever it is applicable, the results presented in these references will be used in the following analyses.

Figures 4(a) and 4(b) show the data asymmetry models that will be considered in the following sections. For NRZ data stream, +1NRZ symbols are elongated by ATJ2 (relative to their nominal value of T_s seconds) when a negative-going data transition occurs and -1 symbols are shortened by the same amount when a positive-going data transition occurs, and the symbols maintain their nominal T_s seconds when no transitions occur. Similarly, For Bi- ϕ data stream, +1Bi- ϕ symbols are elongated by ATJ4 (relative to their nominal value of TJ2 seconds) when a negative-going data transition occurs and -1 symbols are shortened by the same amount when a positive-going data transition occurs, and the symbols maintain their nominal TJ2 seconds when no transitions occur.

3.1 The Effects of Data Asymmetry on PCM/PM/NRZ System Performance

The impact of NRZ data asymmetry on the performance of a space telemetry system that employed PCM/PSK/PM modulation has been investigated in [6]. Since PCM/PSK/PM uses the subcarrier to separate the data from the RF residual carrier, the interference from the data to the carrier tracking is neglected in [6]. This section will extend the results presented in [6] to include PCM/PM/NRZ signal format.

For the data asymmetry model shown in Figure 4(a) and for a purely random and equiprobable NRZ data (i.e., perfectly balanced NRZ data stream), the conditional average probability of error associated with hard decision made on the in-phase integrate-and-dump output of the symbol synchronizer can be shown to have the following form (using Eqn. (5) and similar technique presented in [7])

$$P_e(\theta_c) = (5/16) \operatorname{erfc}\{\sqrt{E_s/N_o}\cos(\theta_c)\} + (1/8) \operatorname{erfc}\{\sqrt{E_s/N_o}(1-\xi)\cos(\theta_c)\} + (1/16) \operatorname{erfc}\{\sqrt{E_s/N_o}(1-2\xi)\cos(\theta_c)\} \quad (13)$$

where ξ denotes the data asymmetry. Here, one has assumed that the carrier tracking is imperfect and the symbol synchronizer operates perfectly.

In order to calculate the average probability of error in Eqn. (6), the variance of the tracking phase error θ^* must be found. Using the linear model for the carrier tracking loop, the variance σ^2 is given by [2]

$$\sigma^2 = 2B_L N / (2P_c) \quad (14)$$

where N is the modified noise spectral density resulting from the thermal noise and NRZ data asymmetry, $2B_L$ is the two-sided loop bandwidth, and P_c is the carrier power equal to $P_c \cos^2(m_T)$.

If we let $H(j2\pi f)$ denote the carrier loop transfer function, the two-sided loop bandwidth and the modified noise spectral density can be written, respectively, as

$$2B_L = \int_{-\infty}^{\infty} |H(2\pi f)|^2 df \quad (15)$$

$$N = (1/2B_L) \int_{-\infty}^{\infty} |H(2\pi f)|^2 [N_o + S_1(f)] df \quad (16)$$

where $S_1(f)$ is the data spectrum that causes the interference to the carrier tracking. In general, for $2B_L \ll R_s$, the interference data spectrum $S_1(f)$ can be written as

$$S_1(f) = P \sin^2(m_T) [S_{dc}(f) + SC(f)] \quad (17)$$

where $S_{dc}(f)$ is the dc component (or the harmonic components) caused by the imperfect

data stream that falls on the RF residual carrier, and $S_c(f)$ is the continuous data spectrum that falls within the carrier tracking loop bandwidth.

Substituting Eqn (16) into Eqn (14) we obtain the variance of the carrier tracking phase error. Assuming $|H(0)|^2 = 1$, we get

$$\sigma^2 = I/p_o + (\alpha/2)\tan^2(m_T) + (1/2)(1/C) \quad (18)$$

where p_o is defined as before, and

$$\alpha = \text{interference due to continuous spectrum} = \int_{-\infty}^{\infty} |H(2\pi f)|^2 S_c(f) df \quad (19)$$

$1/C$ = Interference caused by dc component-to-carrier-power ratio

$$= \tan^2(m_T) \int_{-\infty}^{\infty} S_{dc}(f) df \quad (20)$$

[6] has derived the power spectral density for the asymmetric NRZ data stream illustrated in Figure 4(a). The dc and continuous spectral components for equiprobable symbols are given by [6]

$$S_{dc}(f) = (1/4)\xi^2 \delta(f) \quad (21)$$

$$S_c(f) = (T_s/8)[\sin^2(\pi f T_s)/(\pi f T_s)^2][3 + 5\cos^2(\pi f T_s \xi)] \\ + (T_s/8)[\sin^2(2\pi f T_s \xi)/(\pi f T_s)^2][3\cos^2(\pi f T_s) + \cos^2(2\pi f T_s \xi)] \quad (22)$$

For this case, we have

$$1/C = (1/4)\xi^2 \tan^2(m_T) \quad (23)$$

and the interference due to continuous spectrum can be computed by substituting Eqn (2,2) into Eqn (19). Having $1/C$ and α we can calculate the variance of the tracking phase error, and hence the pdf of the tracking phase error is completely characterized. Using the resultant pdf together with Eqn (13), the average error probability can be calculated using Eqn (6). The numerical results are plotted in Figures 5a and 5b for the second order Phase-Locked Loop (PLL) with the loop transfer function given by [9]

$$|H(j2\pi f)|^2 = [1 + 2(f/f_n)]/[1 + (f/f_n)] \quad (24)$$

The loop transfer function given in Eqn. (24) is for a particular case when the damping factor β is equal to 0.707. The loop natural frequency f_n for this case is related to the two-sided loop bandwidth $2B_L$ through

$$2B_L = 2\pi f_n[\beta + 1/(4\beta)]. \quad (25)$$

A typical value for modulation index (m_1) of 1.25 rad are used in the computation of the effective carrier loop SNR and average SER shown in Figures 5a and 5b, respectively. The two-sided loop bandwidth-to-symbol rate ratio ($2B_L/R_s$) of 0.001 is chosen in this computation because it has been shown in [4] that the performance of PCM/PM/NRZ will approach ideal BPSK when $2B_L/R_s \leq 0.001$. Figure 5a illustrates the effective carrier loop SNR as a function of symbol SNR for various values of data asymmetry. When plotting Figure 5a one assumes that the carrier loop operates in the linear region so that the loop SNR is inversely proportional to the variance of the tracking phase error. Figure 5b shows that the symbol SNR degradation for PCM/PM/NRZ is between 0.2 dB to 0.25 dB for $10^{-8} < \text{SER} < 10^{-7}$, and data asymmetry (ξ) of 6% and about 0.1 dB or less when $\xi = 2\%$.

3.2 The Effects of Data Asymmetry on PCM/PM/Bi- ϕ System Performance

[8] has analyzed the effects of Bi- ϕ data asymmetry on the space telemetry performance degradation. The average probability of error conditioned on the carrier phase error is found to be [8]

$$P_e(\theta_e) = (1/4) [\text{erfc}\{\sqrt{E_s/N_o}(1-\xi)\cos(\theta_e)\} + \text{erfc}\{\sqrt{E_s/N_o}(1-\xi/2)\cos(\theta_e)\}] \quad (26)$$

Based on the data asymmetry model shown in Figure 4(b), the power spectral density for a balanced Bi- ϕ data stream has been derived in [8], and consequently, we can show that the interference caused by dc component-to-carrier-power ratio and the continuous spectral component are given by, respectively

$$I/C = (9/4)\xi^2 \tan^2(m_T) \quad (27)$$

$$\begin{aligned} S_c(f) = & T_s(\pi f T_s/2)^2 C_6(\xi) \sin^2[\pi f T_s(1+\xi)/2] \\ & + T_s(\pi f T_s/2)^2 C_7(\xi) \sin^2[\pi f T_s(1-\xi)/2] + T_s(\pi f T_s)^2 \sin^4[\pi f T_s/2] \\ & - T_s(\pi f T_s/2)^2 [C_1(\xi) + C_2(\xi) + C_3(\xi)] \sin^2[\pi f T_s \xi] \\ & - T_s(\pi f T_s/2)^2 C_4(\xi) \sin^2[\pi f T_s \xi/2] - T_s(\pi f T_s/2)^2 C_5(\xi) \sin^2[\pi f T_s \xi/2] \end{aligned} \quad (28)$$

The parameters $C_1(\xi)$ - $C_7(\xi)$ found in Eqn (28) are defined as follows:

$$C_1(\xi) = (1/4) \sin^2[\pi f T_s(1+\xi)/2] \{ \sin^2[\pi f T_s(1-\xi)/2] + \cos(\pi \xi f T_s) \} \quad (29)$$

$$C_2(\xi) = (1/8) \cos^2[\pi f T_s \xi] \{ 2 \sin^2[\pi f T_s(1-\xi)/2] - \sin^2(\pi \xi f T_s/2) \} \quad (30)$$

$$C_3(\xi) = (1/8) [1 - 4 \cos(\pi f T_s/4)] \quad (31)$$

$$C_4(\xi) = (1/8) \sin[\pi f T_s \xi] \sin[\pi f T_s \xi/2] + \sin[5\pi \xi f T_s/2] \sin[\pi f T_s \xi] \{ 1 - \cos(\pi f T_s) \cos(\pi f T_s \xi) \}. \quad (32)$$

$$C_5(\xi) = -(3/8)\sin[\pi f T_s/4] \sin[\pi f T_s \xi/4] + (1/S) \{2\cos[3\pi \xi f T_s] - \cos[2\pi \xi f T_s]\} \quad (33)$$

$$C_6(\xi) = (1/8) \{ \sin^2[\pi f T_s(1 - \xi)/2] - (3/2)\sin^2[\pi f T_s(1 + \xi)/2] \} \quad (34)$$

$$C_7(\xi) = (3/16)\sin^2[\pi f T_s(1 - \xi)/2] + (1/4)\sin^2[\pi f T_s \xi/2] \cos(\pi \xi f T_s) \quad (35)$$

The interference due to continuous spectrum, α , can be calculated by substituting Eqn. (28) into Eqn. (19). Again, after calculating I/C and α we can obtain the variance of the tracking phase error and hence the average probability, using Eqns. (18), (8), (26) and (6). The numerical results are plotted in Figures 6a and 6b for the second order PLL with the transfer function given by Eqn (24). Figure 6a plots the effective carrier loop SNR as a function of symbol SNR with data asymmetry as a parameter. Figure 6b shows the SER as a function of symbol SNR for various values of data asymmetry and modulation index of 1.25 rad, $2B_1/R_s = 0.001$. The symbol SNR degradation for PCM/PM/Bi- ϕ obtained from this figure is between 0.67 dB to 0.87 dB for $10^{-5} \leq \text{SER} \leq 10^{-7}$, and data asymmetry of 6%. Note that in order to compare the results presented in Figure 6b with those in Figure 5b for NRZ data, use equal amounts of asymmetry as measured by the actual time displacement of both waveforms transitions. For a fair comparison, one replaces ξ (data asymmetry) in Figure 6b by 2ξ when compared with Figure 5b. As an example, the SER curve for PCM/PM/NRZ operating at 2 % data asymmetry shown in Figure 5b corresponds to the 4 % data asymmetry curve for PCM/PM/Bi- ϕ shown in Figure 6b.

4. The Effects of Unbalanced Data Stream

As in the case for the data asymmetry, the imbalances between + 1's and -1's in the data stream can also cause undesired spectral components at the output of the spacecraft's transmitter. These undesired components can potentially degrade the performance of the space telemetry system. Sections 4.1 and 4.2 will analyze the effects of unbalanced data stream on the performance degradation of PCM/PM systems with NRZ and Bi- ϕ data formats, respectively.

4.1 The Effects of Unbalanced Data Stream on PCM/PM/NRZ System Performance

Recall from the previous sections that in order to calculate the average probability of error (Eqn (6)) one needs to determine the conditional probability of error $P_e(\theta_e)$ and the tracking variance σ^2 . This is because one postulates a Gaussian density for the tracking phase error (Eqn (8)). Using Eqn (5) one can show that the conditional probability of error is the same as Eqn (7) for the case of ideal data stream. Therefore, the problem remains is to evaluate the tracking variance.

The tracking variance for this case can also be calculated using Eqn (18). To evaluate this equation one needs to have the power spectral density for the unbalanced NRZ data stream. The dc and continuous components for unbalanced NRZ data stream are found to be [2]

$$S_{dc}(f) = (1 - 2p)^2 \delta(f) \quad (36)$$

$$SC(f) = 4T_s p(1-p) [\sin^2(\pi f T_s) / (\pi f T_s)^2] \quad (37)$$

where p is the probability of transmitting a -1 pulse or probability of mark. For unbalanced data stream, $p \neq 1/2$. Note that for purely random NRZ data source, the transition density p_t can easily be verified to be $2p(1-p)$.

Using Eqns (19) and (20) one can show that the interferences due to continuous spectrum and dc component have the following forms:

$$I/C = (1 - 2p)^2 \tan^2(m_T) \quad (38)$$

$$\alpha = 4T_s p(1-p) \int_{-\infty}^{\infty} |H(2\pi f)|^2 [\sin^2(\pi f T_s) / (\pi f T_s)^2] \quad (39)$$

Substituting Eqns (38) and (39) into Eqn (18) one obtains the tracking variance for this case and hence the pdf for the tracking phase error $P(\theta_e)$ is completely characterized. Substituting the resultant pdf and Eqn (7) into Eqn (6) one obtains an expression for the average probability of error for an unbalanced NRZ data stream. This average error probability is calculated as a function of symbol SNR for various values of p and modulation index m_T , and the results are plotted in Figures 7a, 7b and 8, respectively. Figure 7a plots the effective carrier loop SNR as a function of symbol SNR for various values of p . Figure 7b shows that the symbol SNR degrades seriously when $p \leq 0.4$ for $m_T = 1.25$ rad and $2B_L/R_s = 0.001$. As we decrease the modulation index the SER performance improves because more power is allocated to the carrier and less to the dc component created by the unbalanced between $+1$'s and -1 's. This improvement is evident from Figure 8.

4.2 The Effects of Unbalanced Data Stream on PCM/PM/Bi- ϕ System Performance

As in Section 4.1, the conditional probability of error can be shown to have the same form as in Eqn (7) for the case of ideal data stream, and the task is to determine the tracking variance. If one assumes $2B_L \ll R_s$ then the dc and continuous components for unbalanced Bi- ϕ data stream can be shown to be [2]

$$S_{dc}(f) = 0 \quad (40)$$

$$S_c(f) = 4T_s p(1-p) [\sin^4(\pi f T_s/2) / (\pi f T_s/2)^2] \quad (41)$$

Therefore, the parameters I/C and α become

$$I/C = 0 \quad (42)$$

$$\alpha = 4T_s p(1-p) \int_{-\infty}^{\infty} |H(2\pi f)|^2 [\sin^4(\pi f T_s/2) / (\pi f T_s/2)^2] \quad (43)$$

Again, substituting Eqns (42) and (43) into Eqn (18) we obtain the tracking variance for this case and hence the pdf for the tracking phase error $P(\theta_e)$. Substituting the resultant pdf and Eqn (7) into Eqn (6) one gets an expression for the average probability of error for an unbalanced Bi- ϕ data stream. The numerical results for the effective carrier loop SNR and the average probability of error are plotted in Figures 9a and 9b, respectively. Both Figure 9a and 9b show that the performance of the PCM/PM/Bi- ϕ receiver is not susceptible to the unbalanced data stream.

5. Behavior of PCM/PM Receivers in the Presence of Band-Limited Channels

When the RF filter bandwidth becomes less than the main spectrum hump of the modulated carrier, the information-bearing pulses are spread out in time. Each pulse is overlaid with the tails of previous pulses and the precursors of the subsequent ones, and this so-called Intersymbol Interference (ISI) behaves like an additional random noise. This additional random noise can cause potential degradation to the receiver. In addition, excessive filtering of the pulse can also cause a loss of bit energy during the bit time. This section will analyze the performance of the PCM/PM receiver in the presence of ISI.

Let $P(t)$ denote the pulse shape of the data and $h(t)$ denote the impulse response of the equivalent low-pass filter of the RF bandpass filter with bandwidth B . The received data can be expressed in term of $P(t)$ and $h(t)$ as follow

$$d(t) = \sum_{k=-\infty}^{\infty} d_k g(t - kT) \quad (44)$$

where $d_k = \pm 1$ with $\Pr\{d_k = +1\} = \Pr\{d_k = -1\} = 1/2$, and $g(t)$ is given by

$$g(t) = P(t) * h(t) \quad (45)$$

where $*$ denotes the convolution.

For this case the symbol energy becomes

$$E_s = P \sin^2(m_T) \int_0^T |g(t)|^2 dt \quad (46)$$

Using Eqn (5) one can show that the output of the integrate-and-dump filter in the presence of the band-limited channel have the following form

$$Z(T) = E_s \left[1 + \sum_{k=-\infty}^{\infty} d_k \lambda_k \right] \cos \theta_e + n(T) \quad (47)$$

where the prime in the sum indicates the omission of the term $k = 0$, and

$$\lambda_k = \frac{\int_0^{T_s} g(t)g(t+kT_s)dt}{\int_0^{T_s} |g(t)|^2 dt} \quad (48)$$

Note that in Eqn (47) one has assumed $d_0 = +1$. Therefore, the conditional probability $P_e(\theta_e)$ of error is then the probability that $Z(T_s) < 0$ when $d_0 = +1$,

$$P_e(\theta_e) = \Pr\{Z(T_s) < 0/\theta_e, d_0 = +1\} \quad (49)$$

Calculating $P_e(\theta_e)$ exactly is very difficult, because one has to take all possible combinations of the digits $d_k = \pm 1$ into account, $1 \leq |k| \leq \infty$. Here one will assume that only a finite number M of pulses before and after d_0 , i.e., one considers only the ISI effects of the M preceding and M subsequent bits on the bit under detection. In order to calculate $P_e(\theta_e)$ exactly for M pulses before and after d_0 one needs to account for 2^{*M} combinations. Since, for accuracy, the value of M selected typically depends on the time-bandwidth product BT_s and the value of M becomes very large when $BT_s \ll 1$; the length of the computation grows exponentially with M . To avoid the complexity associated with this technique for large M , Helstrom [10] has shown that this conditional error probability $P_e(\theta_e)$ can be evaluated by numerical quadrature of a Laplace inversion integral along a contour in the complex plane passing through a saddlepoint of the integrand. For finite M , the amount of computation associated with this technique only increases linearly with M .

For $BT_s \geq 1$, the value of $1 \leq M \leq 2$ is sufficient. When M is small, direct computation of the conditional error probability $P_e(\theta_e)$ is feasible through the following equation

$$P_e(\theta_e) = (1/2) \left[(1/2^{2M}) \sum_{\substack{k=2^{2M} \\ \text{combinations}}} \text{erfc}\{\sqrt{E_s/N_0}[1 + \sum' d_k \lambda_k] \cos \theta_e\} \right] \quad (50)$$

As an example, for $M = 1$, Eqn (50) becomes

$$P_e(\theta_e) = (1/2) \left[(1/4) \text{erfc}\{\sqrt{E_s/N_0}(1 + \lambda_{-1} + \lambda_{+1}) \cos \theta_e\} - (1/4) \text{erfc}\{\sqrt{E_s/N_0}(1 + \lambda_{-1} - \lambda_{+1}) \cos \theta_e\} \right. \\ \left. + (1/4) \text{erfc}\{\sqrt{E_s/N_0}(1 - \lambda_{-1} + \lambda_{+1}) \cos \theta_e\} + (1/4) \text{erfc}\{\sqrt{E_s/N_0}(1 - \lambda_{-1} - \lambda_{+1}) \cos \theta_e\} \right] \quad (51)$$

To simplify the computation one will assume ideal bandpass filter so that the transfer function for the equivalent low-pass filter is given by

$$H(f) = \begin{cases} 1, & -B < f < B \\ 0, & \text{elsewhere} \end{cases} \quad (52)$$

The impulse response $h(t)$ is found to be

$$h(t) = 2B \operatorname{sinc}(2Bt) \quad (53)$$

where $\operatorname{sinc}(x) = \sin(\pi x)/(\pi x)$.

Thus, for ideal lowpass filter and perfect data stream, the output of the filter $g(t)$ can be obtained by substituting Eqn (53) into (45). For NRZ data format, $g_{\text{NRZ}}(t+kT_s)$ can be shown to be

$$g_{\text{NRZ}}(t+kT_s) = \frac{1}{\pi} [\operatorname{si}\{2\pi B(t+T_s(k+1/2))\} - \operatorname{si}\{2\pi B(t+T_s(k-1/2))\}] \quad (54)$$

For Bi- ϕ data format one gets

$$g_{\text{Bi-}\phi}(t+kT_s) = \frac{1}{\pi} [\operatorname{si}\{2\pi B(t+T_s(k+1/2))\} + \operatorname{si}\{2\pi B(t+T_s(k-1/2))\} - 2\operatorname{si}(2\pi B(t+kT_s))] \quad (55)$$

where

$$\operatorname{si}(x) = \int_0^x [\sin(u)/u] du \quad (56)$$

Substituting Eqns (54) and (55) into Eqn (48) one can calculate λ_k for NRZ and Bi- ϕ data formats, respectively. Therefore, for $1 < M \leq 2$, one can obtain the average error probability P_e by substituting Eqns (8) and (50) into Eqn (6) and performing the numerical integration in a digital computer. Note that the variances of the carrier tracking phase error used in these calculations are given by Eqns (9) and (10) for NRZ and Bi- ϕ data formats, respectively. The numerical results are plotted in Figures 10 and 11 for PCM/PM/NRZ and PCM/PM/Bi- ϕ , respectively. Again, the results shown in these figures are for $m_1 = 1.25$ rad and $2B_1/R_s = 0.001$. As expected, these numerical results show that the PCM/PM/NRZ outperforms PCM/PM/Bi- ϕ in the presence of ISI caused by band-limited channel.

6. Numerical Results and Discussions

Figures 12-14 show the performance comparison between PCM/PM/NRZ and PCM/PM/Bi- ϕ in the presence of data asymmetry, unbalanced data stream and bandlimiting channel, respectively. Figure 12 shows that for fixed modulation index, $2B_1/R_s$ and data asymmetry, the symbol error probability for PCM/PM/NRZ is superior than that of PCM/PM/Bi- ϕ . This phenomenon can be explained as follow. As shown in Figure 1, the

Bi- ϕ data stream is derived from the NRZ data stream, hence the amount of data asymmetry inherent in the Bi- ϕ data stream will be twice that of NRZ. This is because the transition in Bi- ϕ data stream is effectively twice that of NRZ. The numerical results show that, for data asymmetry less than or equal to 2 %, the symbol SNR degradation is at the order of 0.1 dB or less for both systems when they operate at typical operating conditions ($m_T = 1.25$ rad and $2B_I/R_s = 0.001$).

Figure 13 compares the performance of PCM/PM/NRZ and PCM/PM/Bi- ϕ in the presence of **unbalanced** data streams. As the probability of transmitting a + 1 pulse, p , deviates from 1/2, the performance of PCM/PM/NRZ **degrades** seriously, and that the **degradation** becomes unacceptable when $p < 0.45$. This is due to the presence of a strong dc component (caused by the unbalanced NRZ data stream) at the carrier. On the other hand, due to the absence of the dc component at the carrier frequency for the unbalanced **bi- ϕ** data, the performance of PCM/PM/Bi- ϕ is insensitive to the amount of unbalanced between + 1's and -1's. The symbol SNR degradation for PCM/PM/Bi- ϕ is about 0.3 dB for $p < 0.4$, $m_T = 1.25$ rad and $2B_I/R_s = 0.001$, and it is expected to be less than 0.3 dB when $m_T < 1.25$ rad.

Figure 14 illustrates the performances of PCM/PM/NRZ and PCM/PM/Bi- ϕ when they operate under bandwidth constraint. For $10^{-5} \leq SER \leq 10^{-7}$, $m_T = 1.25$ rad and $2B_I/R_s = 0.001$, the symbol SNR degradation of PCM/PM/NRZ is at the order of 1-1.2 dB for $BT_s = 1$, and less than 0.3 dB for $BT_s = 2$. Under the same operating conditions, the performance degradation of the PCM/PM/Bi- ϕ is unacceptable for $BT_s = 1$, and more than 0.6 dB for $BT_s = 2$. Therefore, the performance of PCM/PM/Bi- ϕ is more susceptible to **bandlimiting** channels than PCM/PM/NRZ.

7. Conclusion

This paper has analyzed and explained the separate effects of data asymmetry, unbalanced data and ISI on the performances of both PCM/PM/NRZ and PCM/PM/Bi- ϕ systems. In the presence of imperfect carrier tracking due to imperfect data stream, it was found that the PCM/PM/Bi- ϕ is sensitive to ISI and data asymmetry. On the other hand, the PCM/PM/NRZ is sensitive to the unbalanced data stream.

Numerical results also indicate that, for typical operating conditions ($m_T = 1.25$ rad, $2B_I/R_s = 0.001$) PCM/PM/NRZ outperforms PCM/PM/Bi- ϕ system in bandlimiting channel as well as in the presence of data asymmetry. In addition, the PCM/PM/Bi- ϕ system is found to be superior than PCM/PM/NRZ when operating under unbalanced data condition, and results also show that the performance degradation of PCM/PM/NRZ becomes unacceptable when the probability of transmitting a + 1 pulse becomes smaller than 0.45. The combined effects of both imperfect data stream and **bandlimiting** channels on the performance of the PCM/PM receivers will be investigated in Part 11 of this paper.

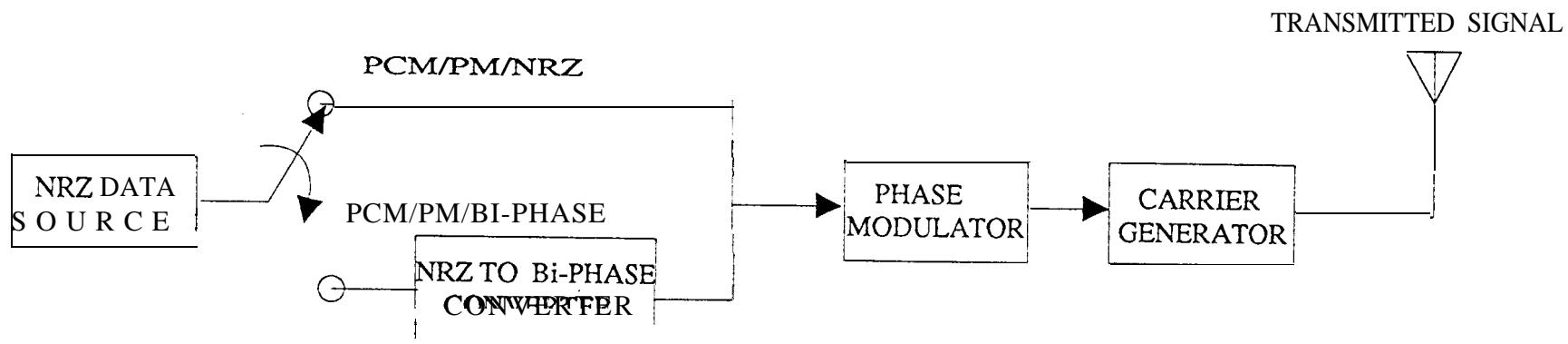
Acknowledgement

The work described in this paper was carried out at the Jet Propulsion Laboratory, California Institute of Technology, under contract with the National Aeronautics and Space Administration.

References

- [1] Consultative Committee for Space Data Systems, Recommendations for Space Data System Standards, Radio Frequency and Modulation Systems, Part I, Earth Stations and Spacecraft, CCSDS 401 .0-B, Blue Book, CCSDS Secretariat, Communications and Data systems Division, (Code OS), NASA, Washington D.C.
- [2] Joe Yuen, editor, Deep Space Telecommunications Systems Engineering, Plenum Press, New York, 1983.
- [3] Tien M. Nguyen, "Closed Form Expressions for Computing the Occupied Bandwidth of PCM/PSK/PM Signals," 1991 IEEE International Symposium on EMC Proceedings, September 1991, Cherry Hills, New Jersey.
- [4] Mazen M. Shihabi, Tien M. Nguyen, Sami M. Hinedi, "On the Use of Subcarriers in Future DSN Missions," the Telecommunications and Data Acquisition Progress Report 42-111, November 15, 1992, NASA, Jet Propulsion Laboratory, Pasadena, California,
- [5] Tien M. Nguyen, "Occupied Bandwidths for PCM/PSK/PM and PCM/PM Signals-A Comparative Study," presented to the International Consultative Committee for Space Data Systems, Subpanel IE, RF and Modulation, Salzburg, Austria, May 1992.
- [6] Tien M. Nguyen, "The impact of NRZ Data Asymmetry on the Performance of a Space Telemetry System," IEEE Transactions on EMC, Vol. 33, No. 4, November 1991.
- [7] W. K. Alem, G. K. Huth, M. K. Simon, "Integrated Source and Channel Encoded Digital Communication System Design Study," Final Report (R7803-7) under Contract NAS 9-15240, Mar. 31, 1978, Axiomatix, Marina del Rey, CA.
- [8] Tien M. Nguyen, "Space Telemetry Degradation clue to Manchester Data Asymmetry Induced Carrier Tracking Phase Error," IEEE Transactions on EMC, Vol. 33, No. 3, August 1991.
- [9] J. K. Holmes, Coherent Spread Spectrum Systems, New York: Wiley-Interscience, 1982, Chapter 4.
- [10] C. W. Helstrom, "Calculating Error Probabilities for Intersymbol and Cochannel Interference," IEEE Transactions on Communication, Vol.COM-34, No.5, May 1986.

TRANSMITTER



RECEIVER

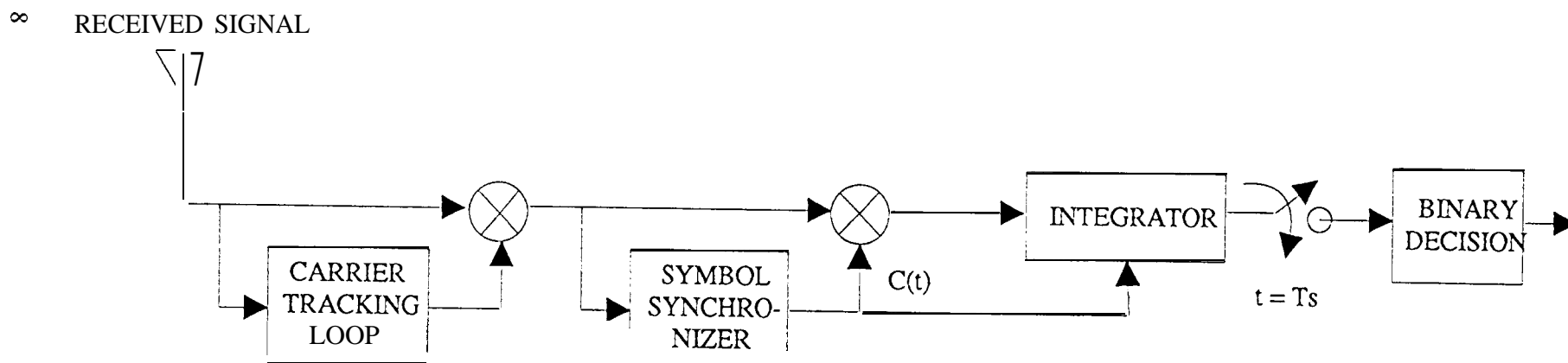
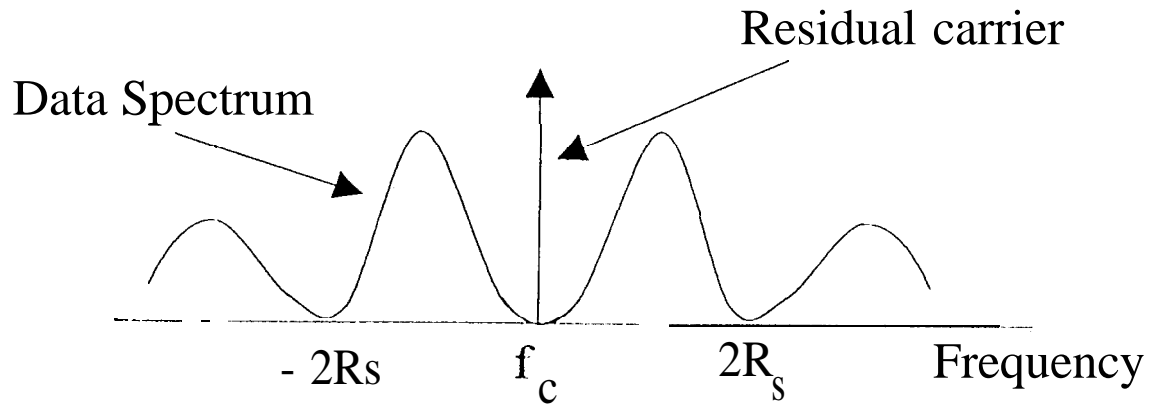
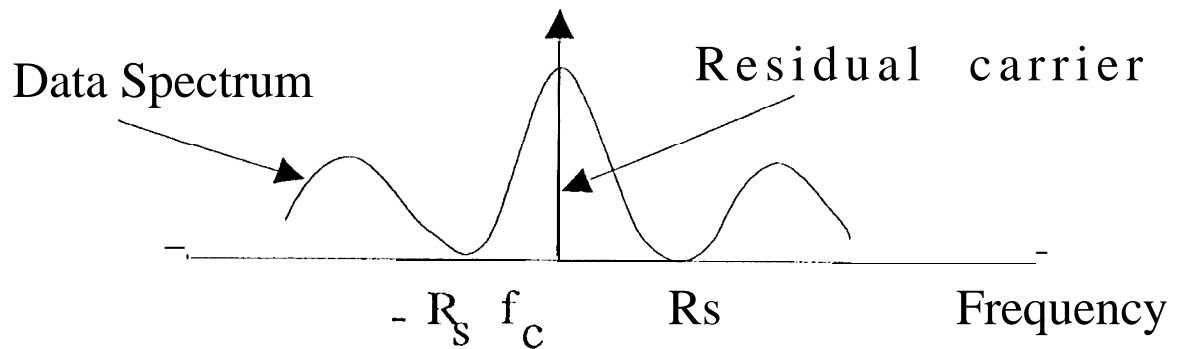


FIGURE 1. SPACE TELEMETRY SYSTEM MODEL

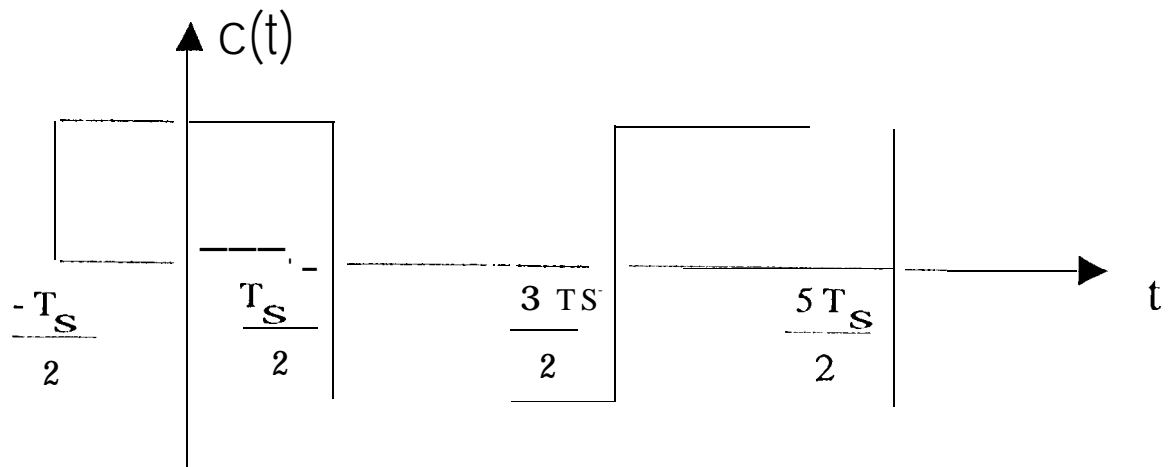


2(a) Power Spectrum of PCM/PM/Bi-Phase Signal

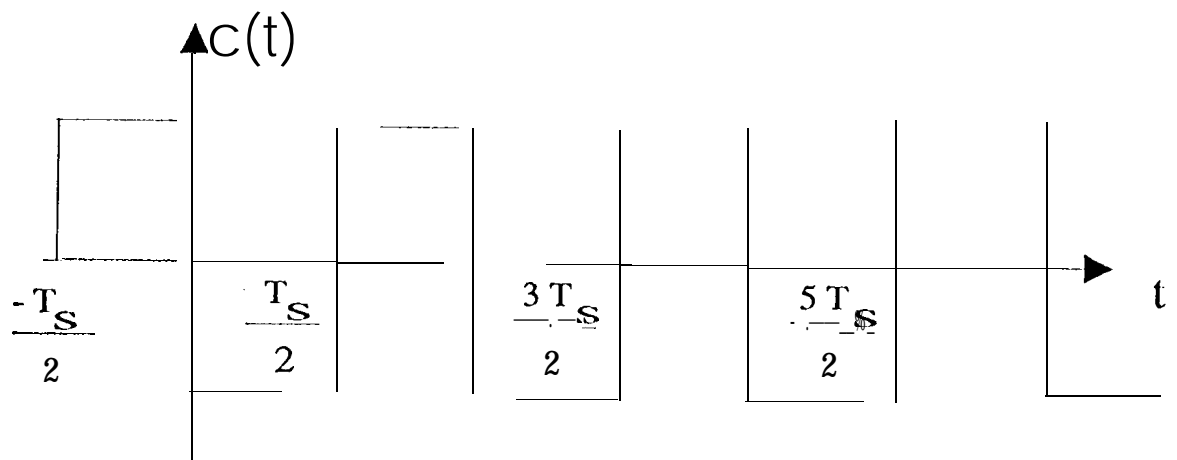


2(b) Power Spectrum of PCM/PM/NRZ Signal

FIGURE 2 POWER SPECTRUM OF PCM/PM SIGNAL

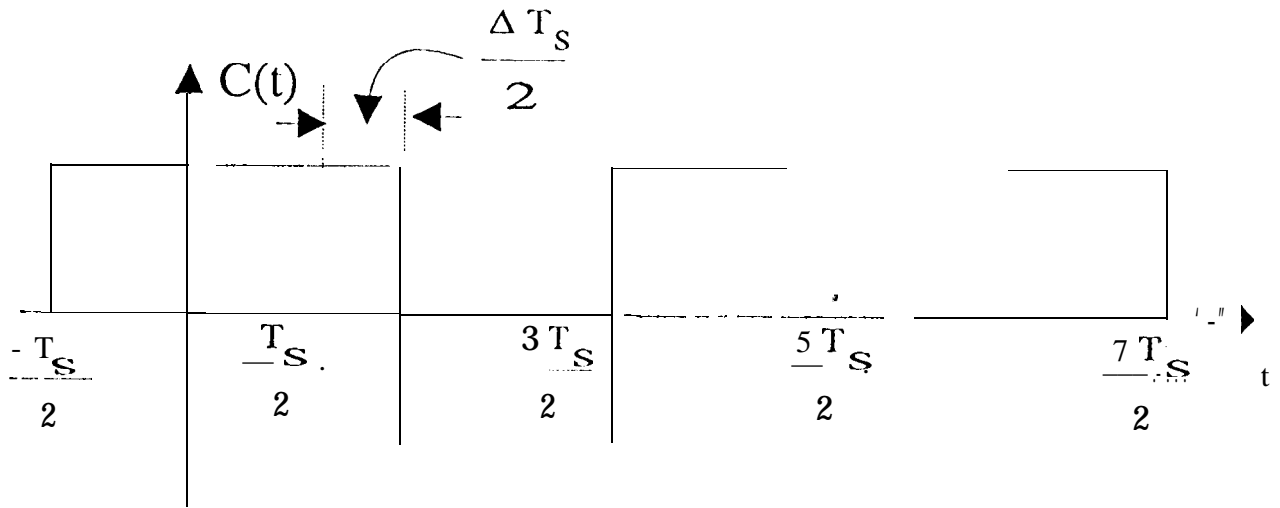


(a) Symbol Sync Clock for NRZ Data

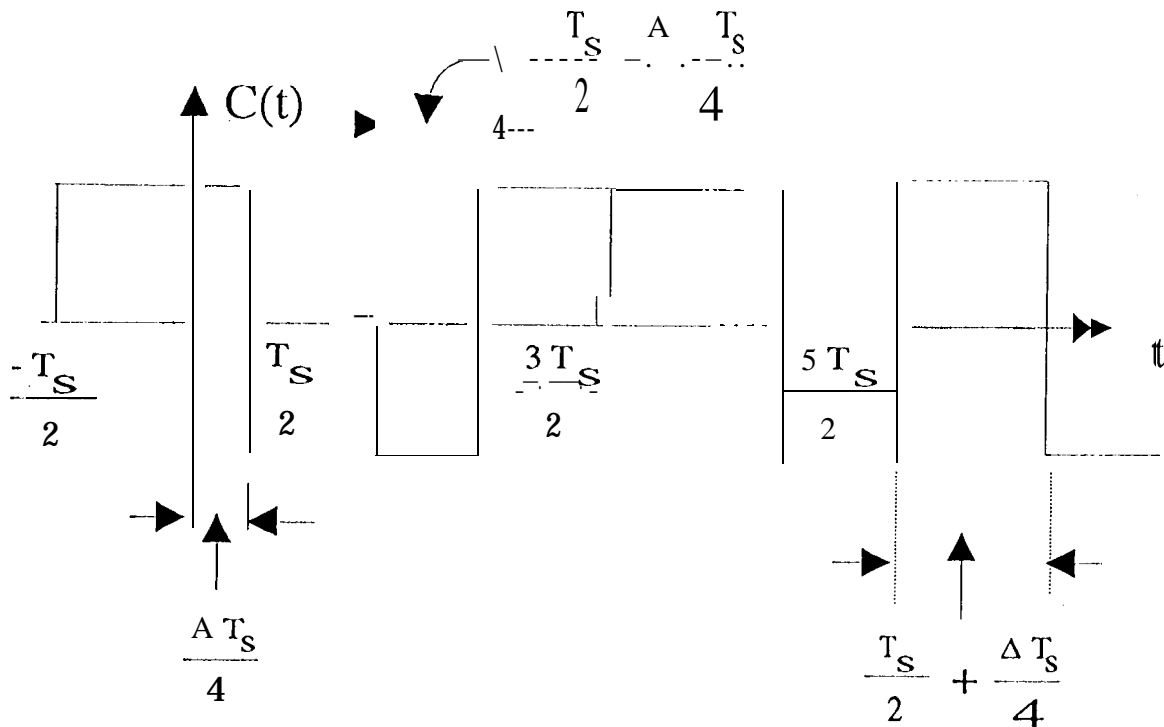


(b) Symbol Sync Clock for Bi-Phase Data

Figure 3. Symbol Sync Clock $C(t)$



(a) Asymmetry Model for NRZ Data Stream



(b) Asymmetry Model for Bi-Phase Data Stream

Figure 4. Asymmetry Models for NRZ and Bi-Phase

Figure 5a. Carrier Loop SNR vs Symbol SNR for Data Asymmetry

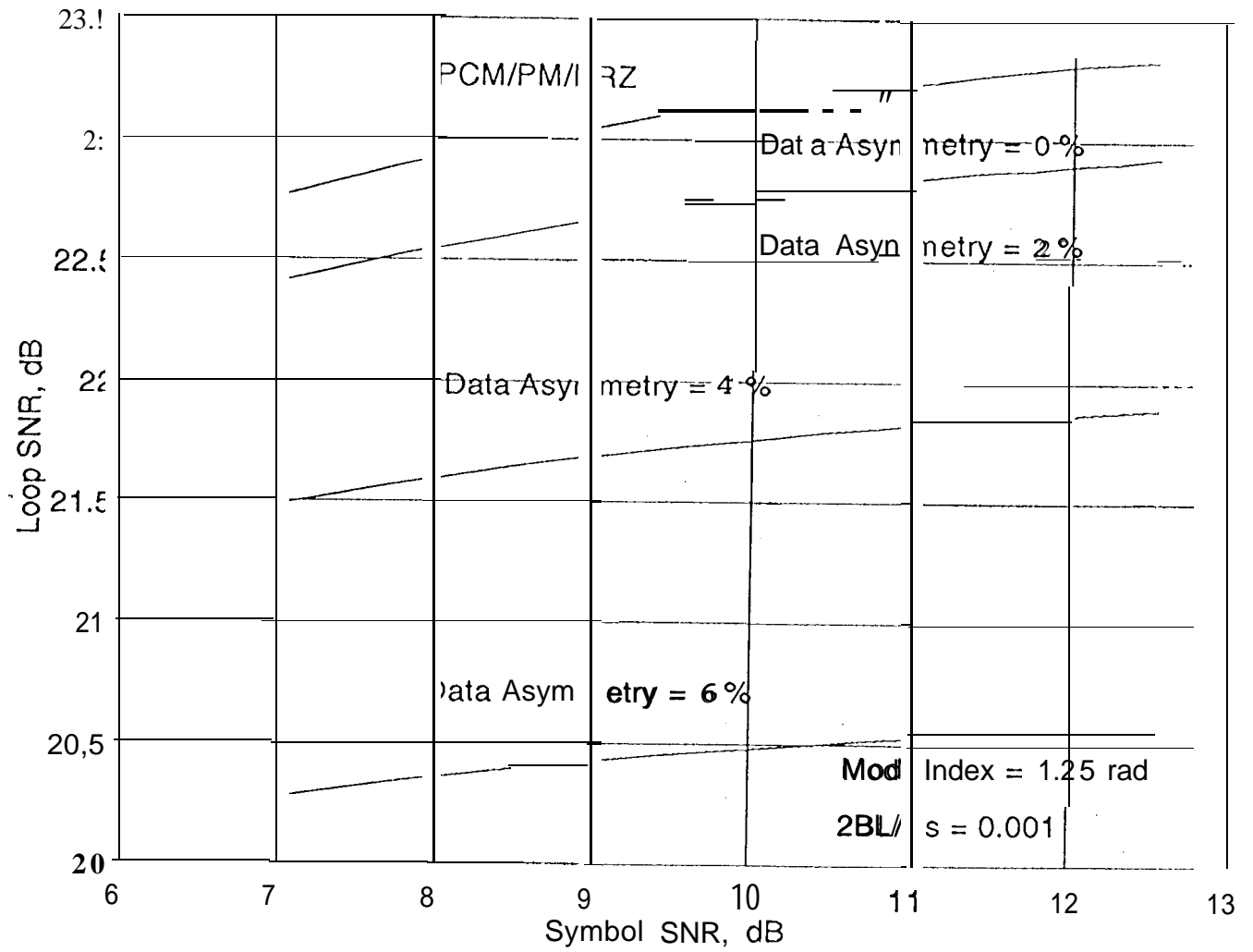
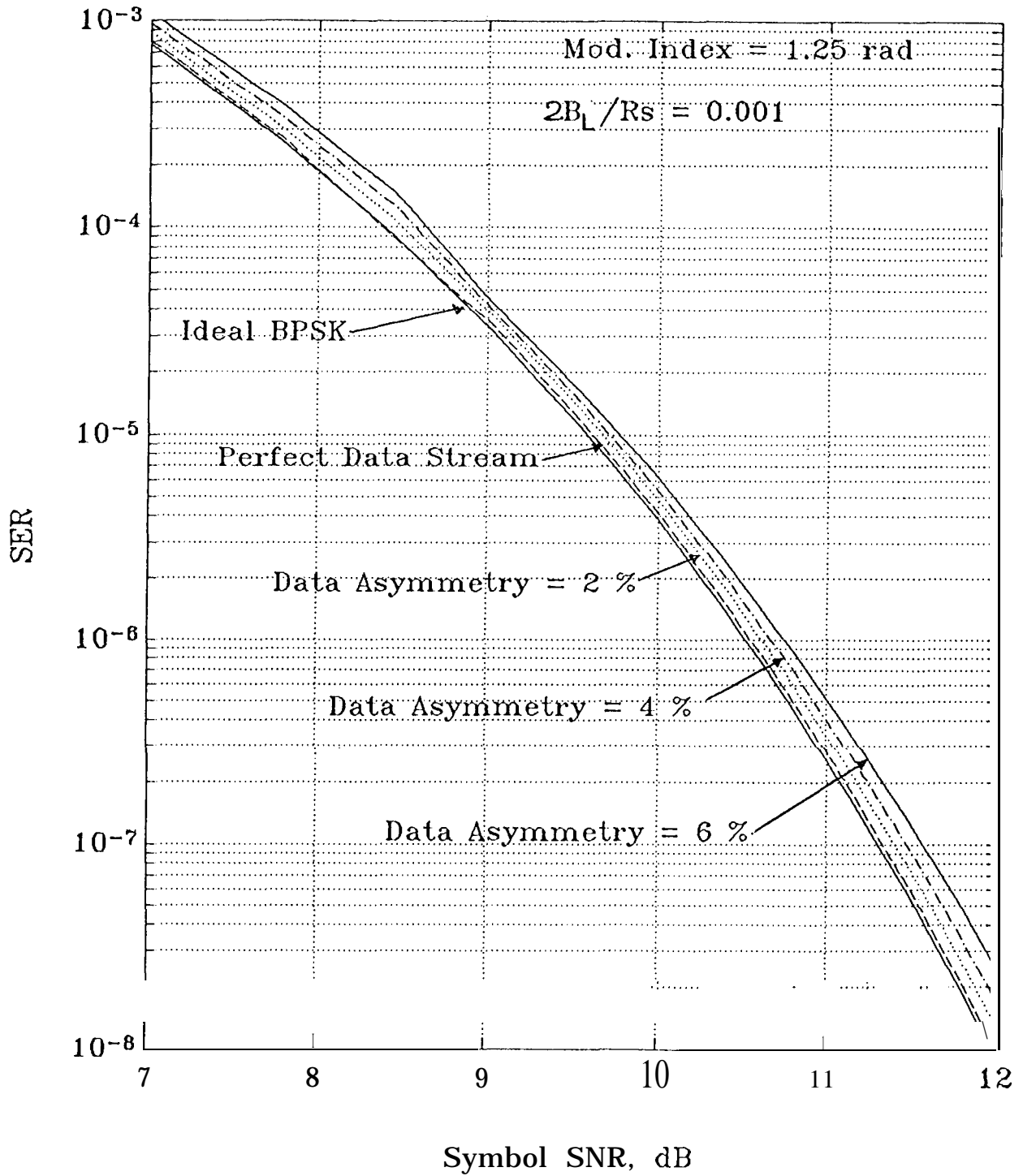


Figure 5b. Performance of PCM/PM/NRZ for Data Asymmetry



PCM/PM/Bi-Phase

Figure 6a. Carrier Loop SNR vs Symbol SNR for Data Asymmetry

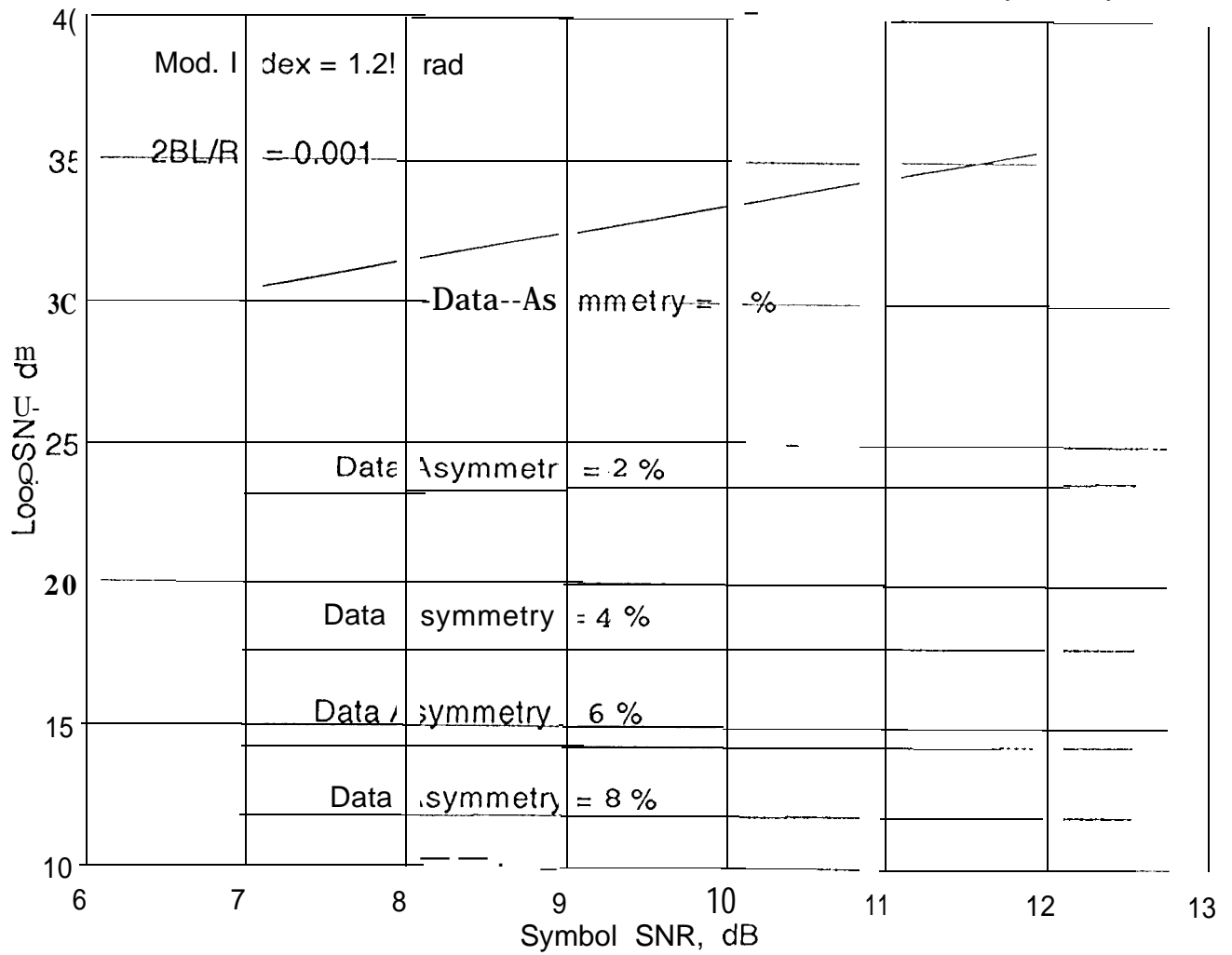


Figure 6b. PCM/PM/Bi-Phase With Data Asymmetry

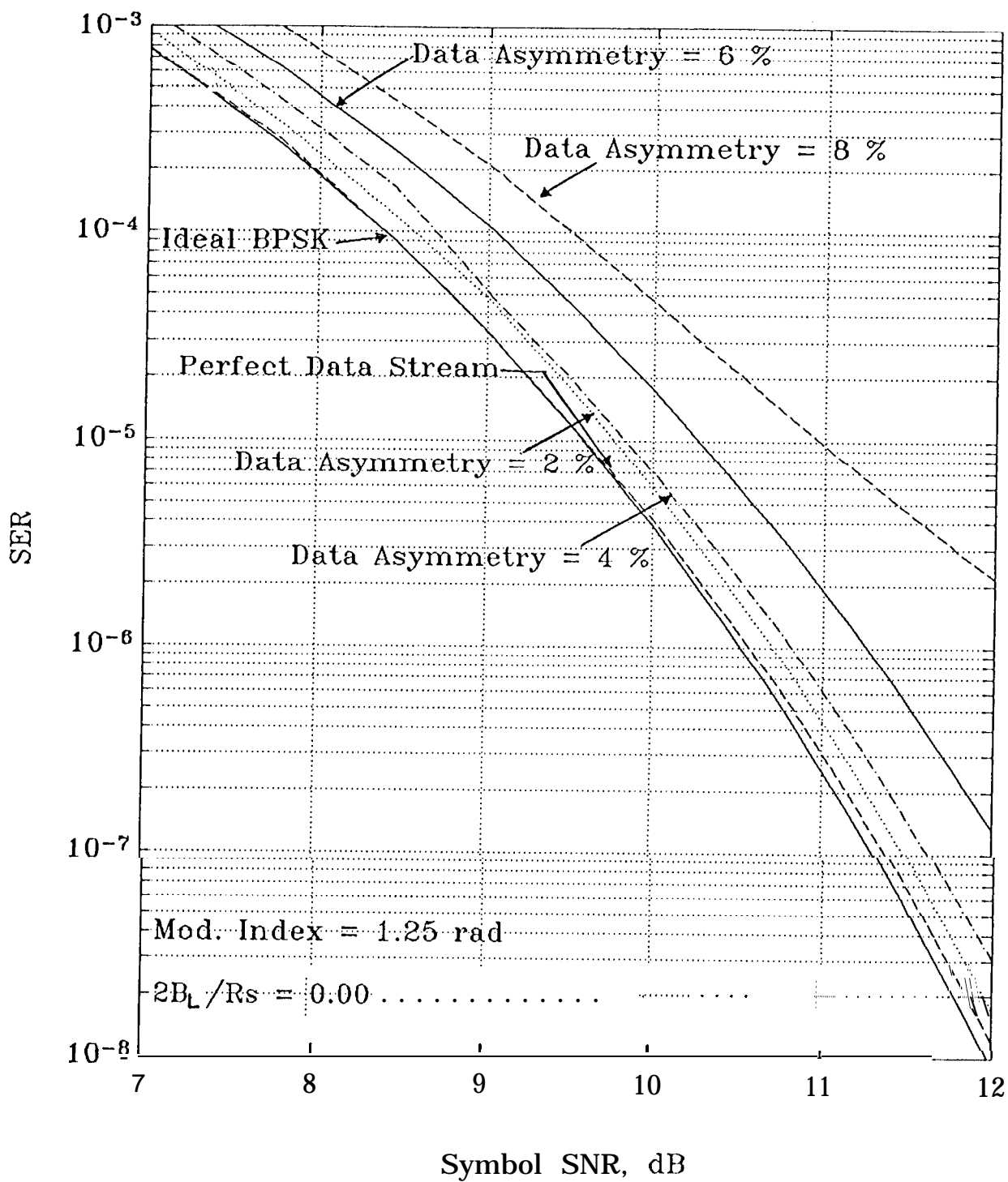


Figure 7a. Carrier Loop SNR vs Symbol SNR for Unbalanced Data

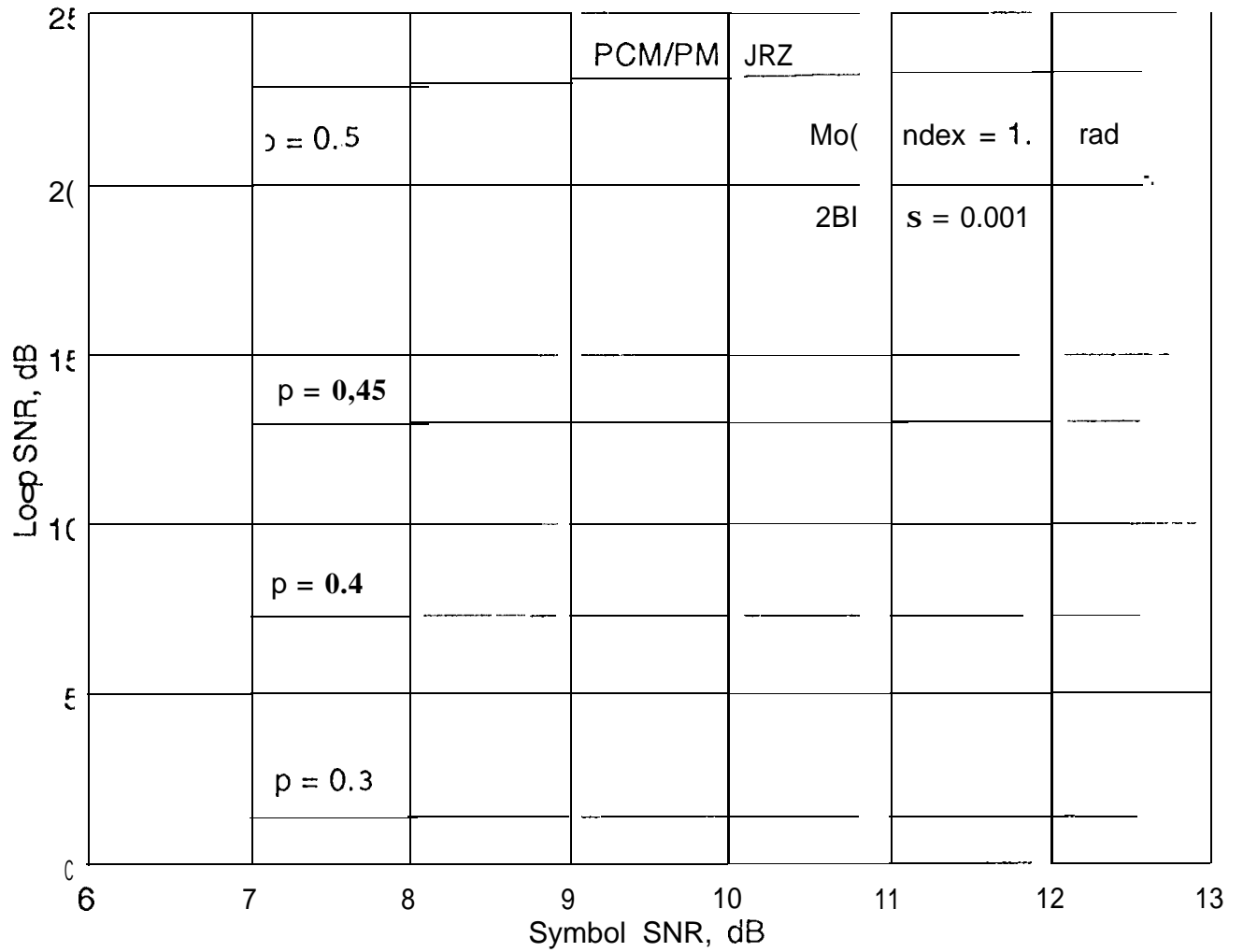


Figure 7b, Performance of PCM/PM/NRZ for Unbalanced Data

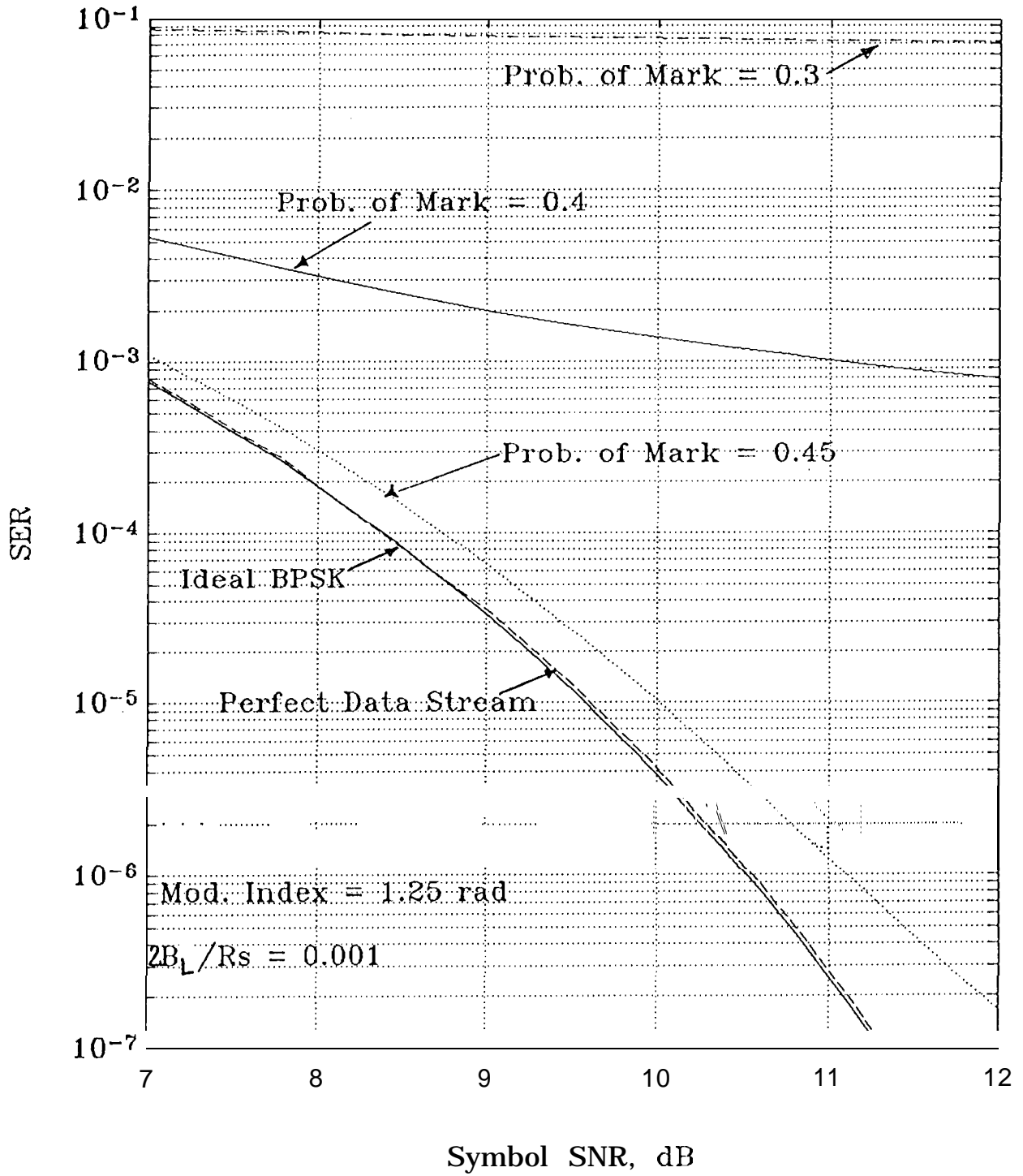


Figure 8. PCM/PM/NRZ With Unbalanced Data

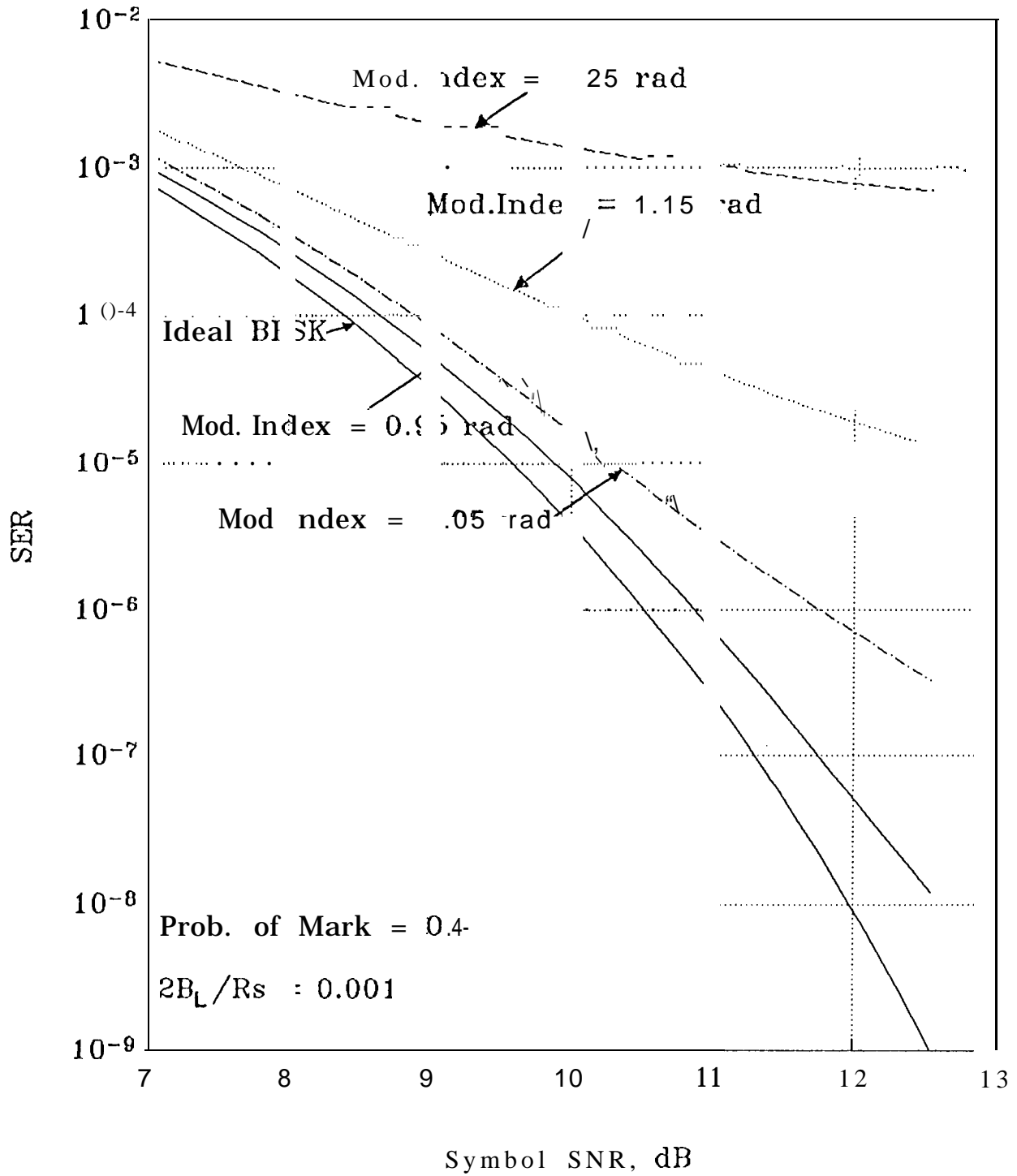


Figure 9a. Carrier Loop SNR vs Symbol SNR for Unbalanced Data

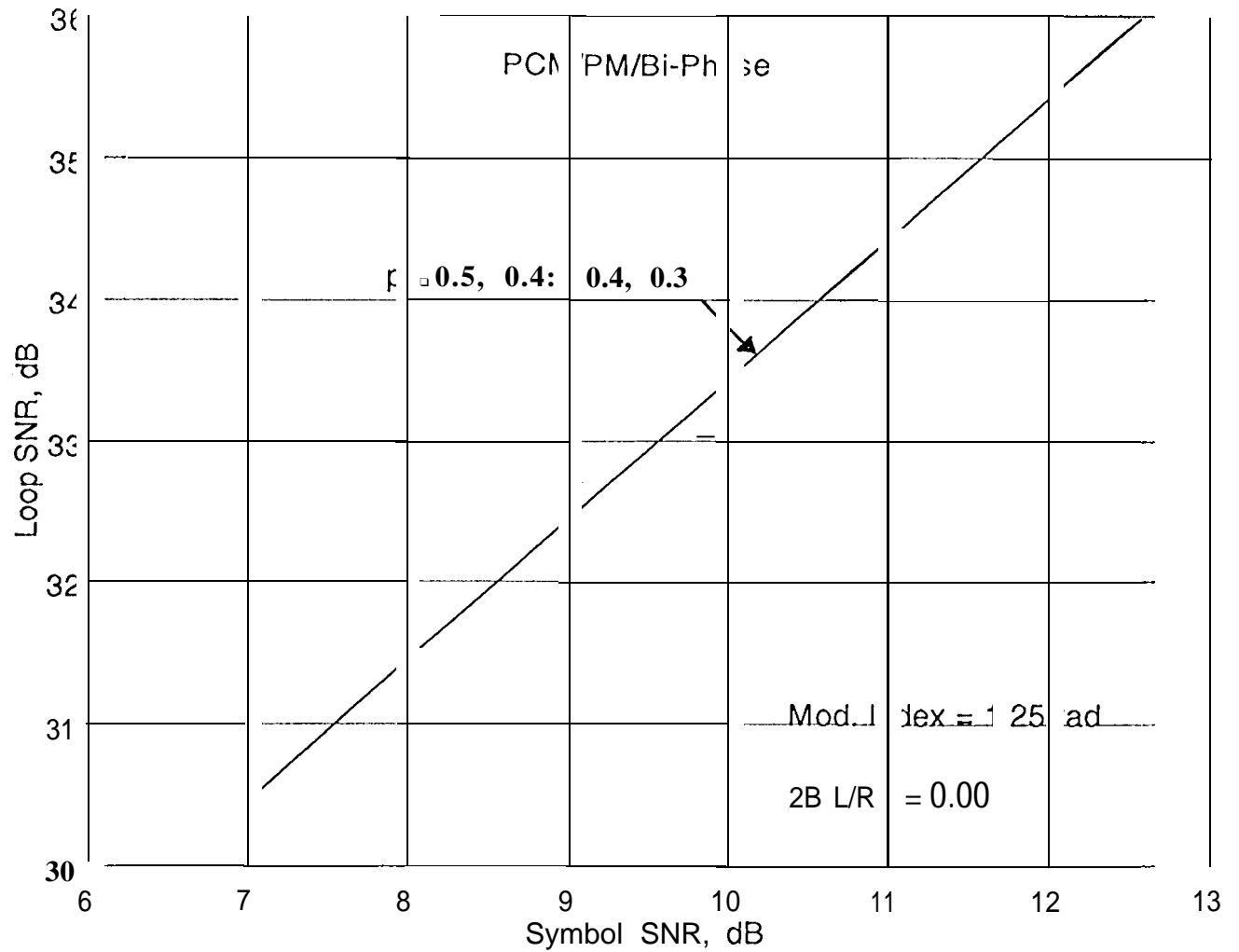


Figure 9b. PCM/PM/Bi-Phase With Unbalanced Data

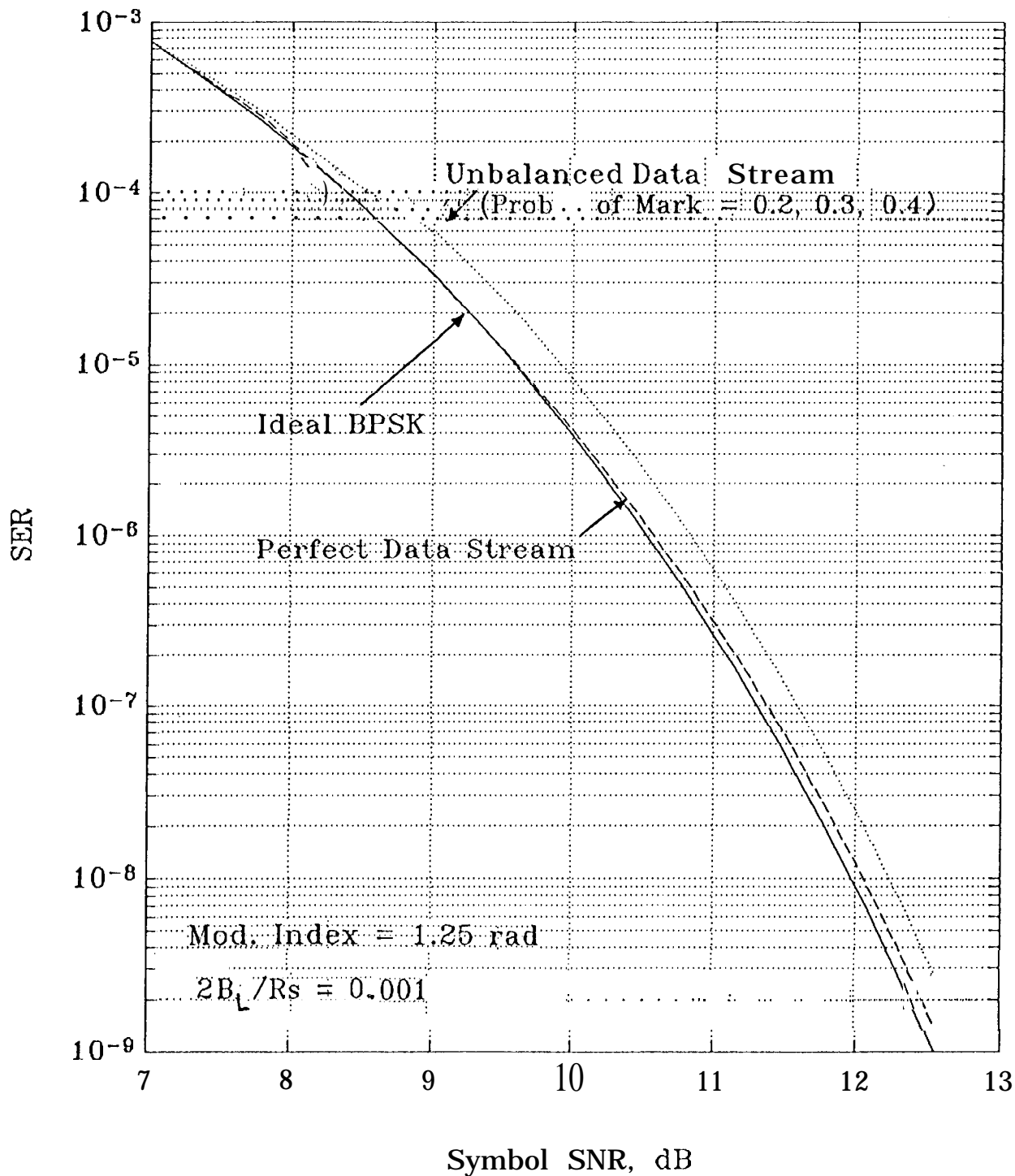


Figure 10. PCM/PM/NRZ With Band-Limited Channel

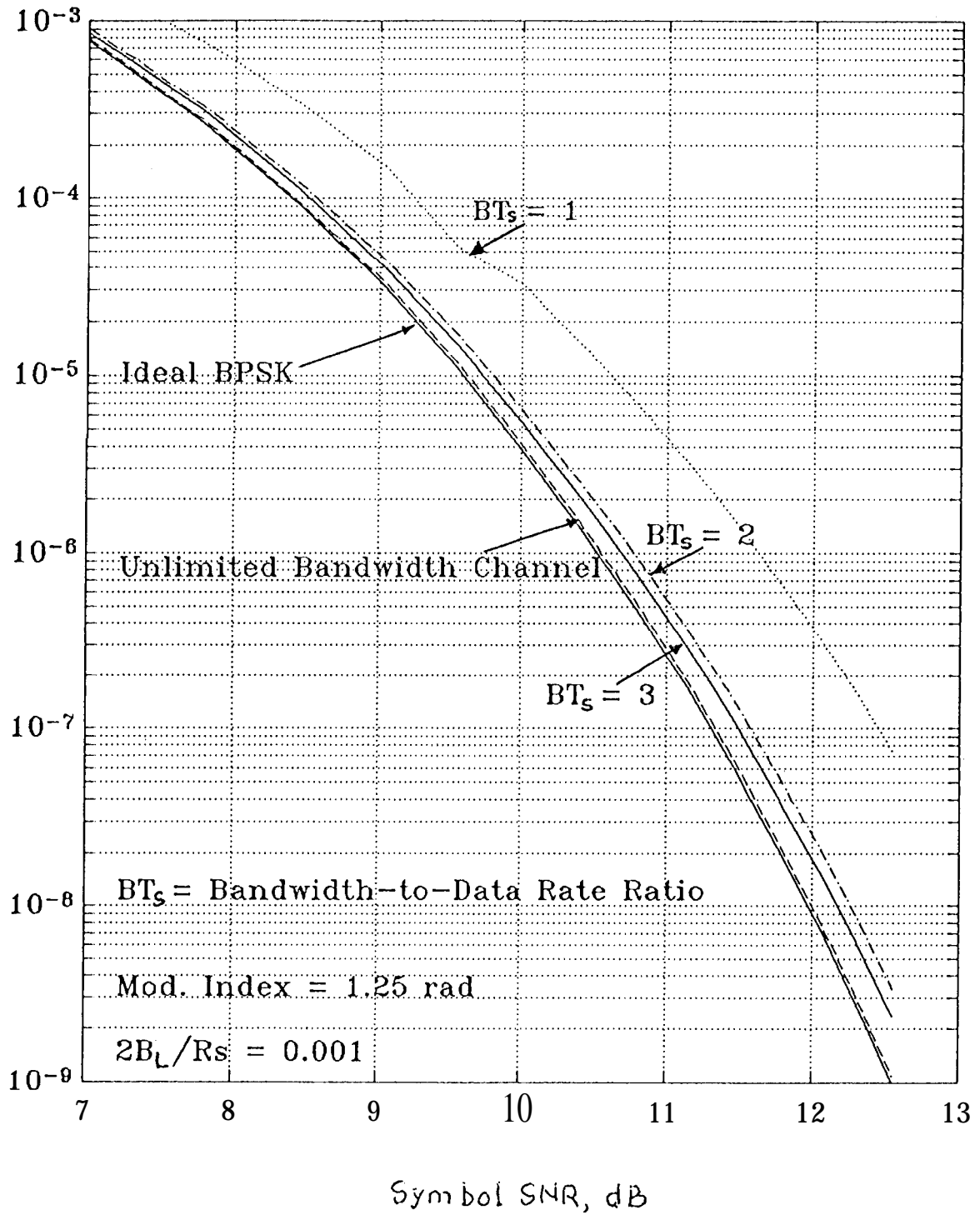


Figure 10. PCM/PM/NRZ With Band -Limited Channel

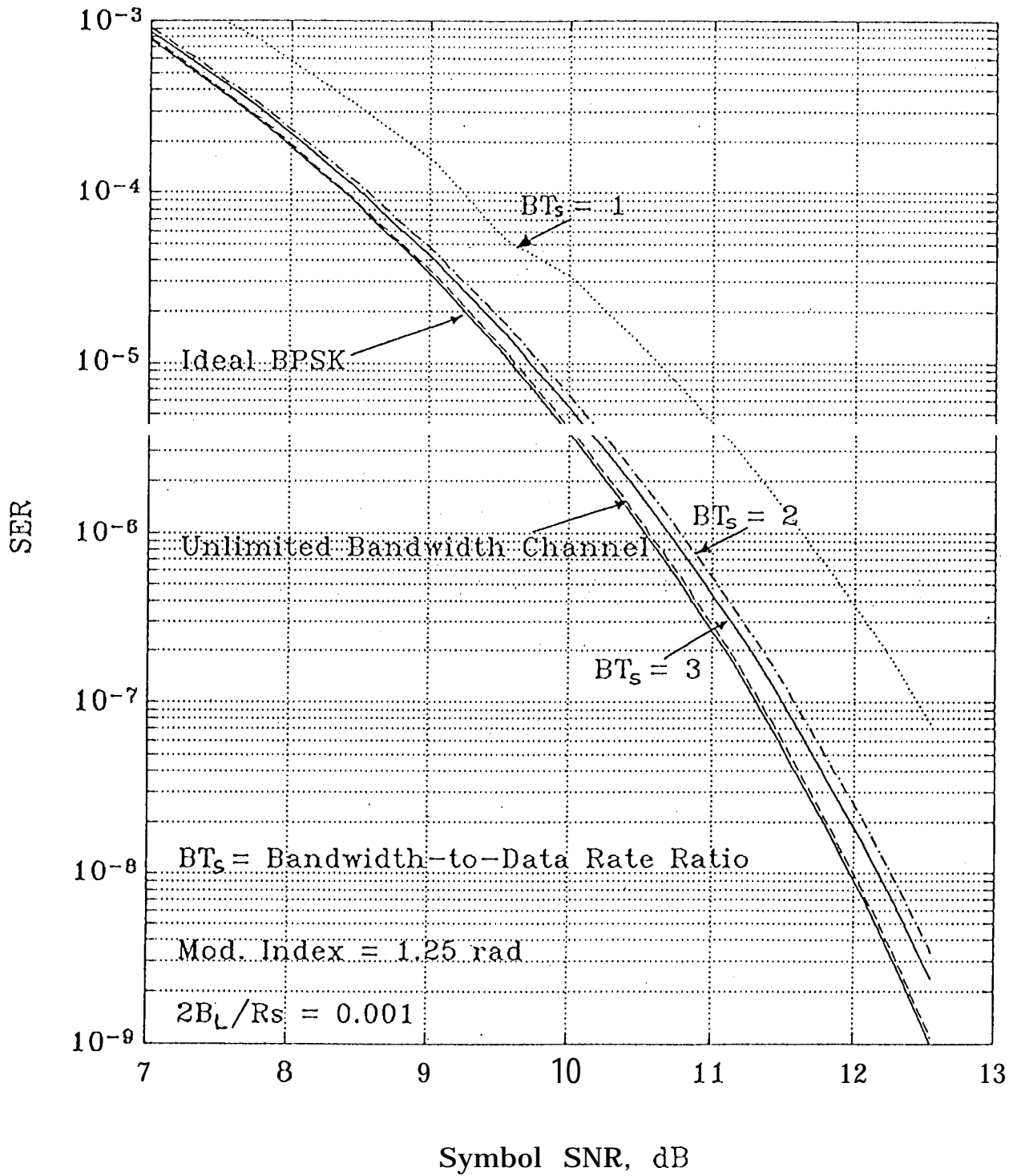


Figure 11. PCM/PM/Bi-Phase With Band-Limited Channel

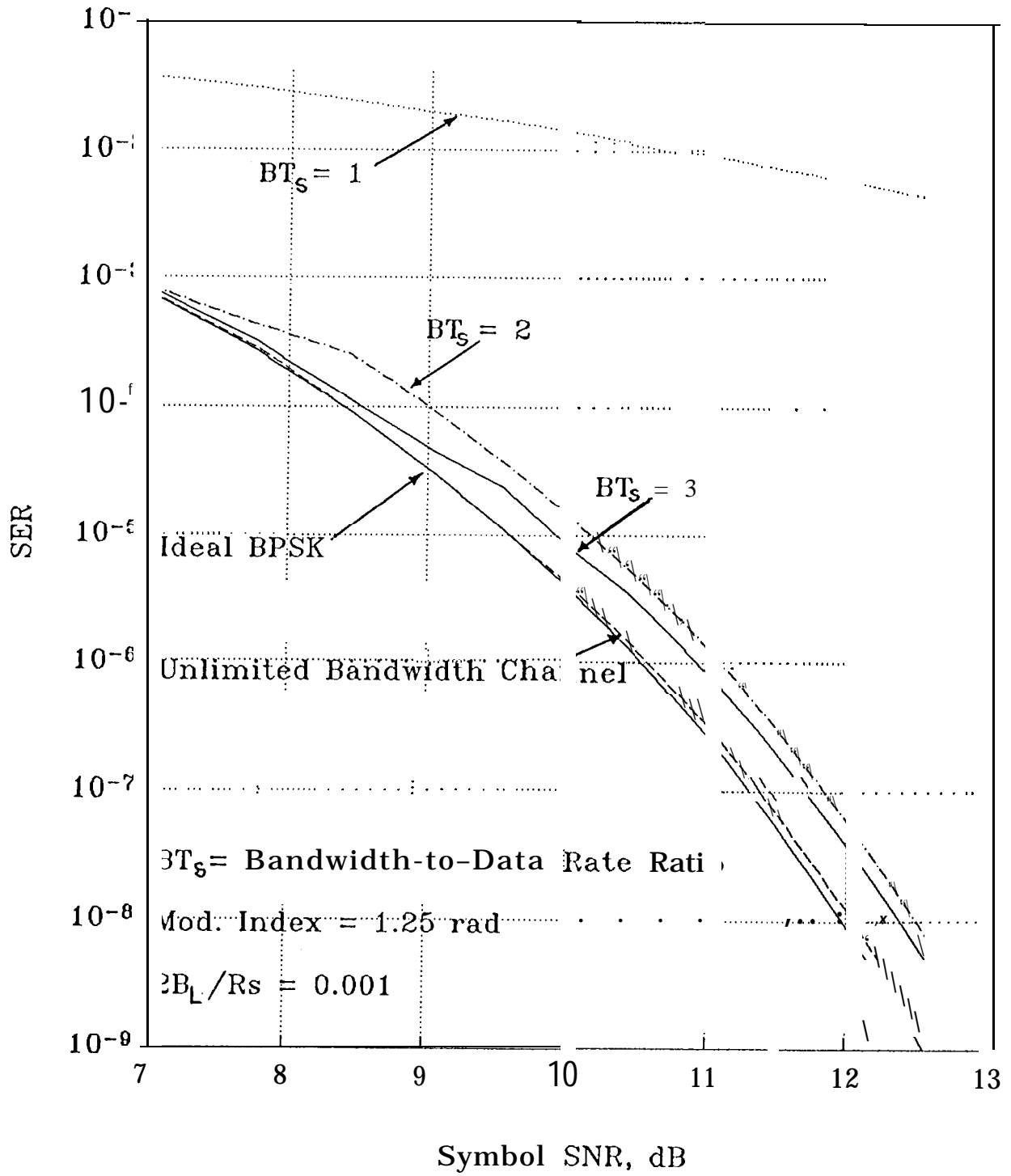


Figure 12. Performance Comparison for Data Asymmetry

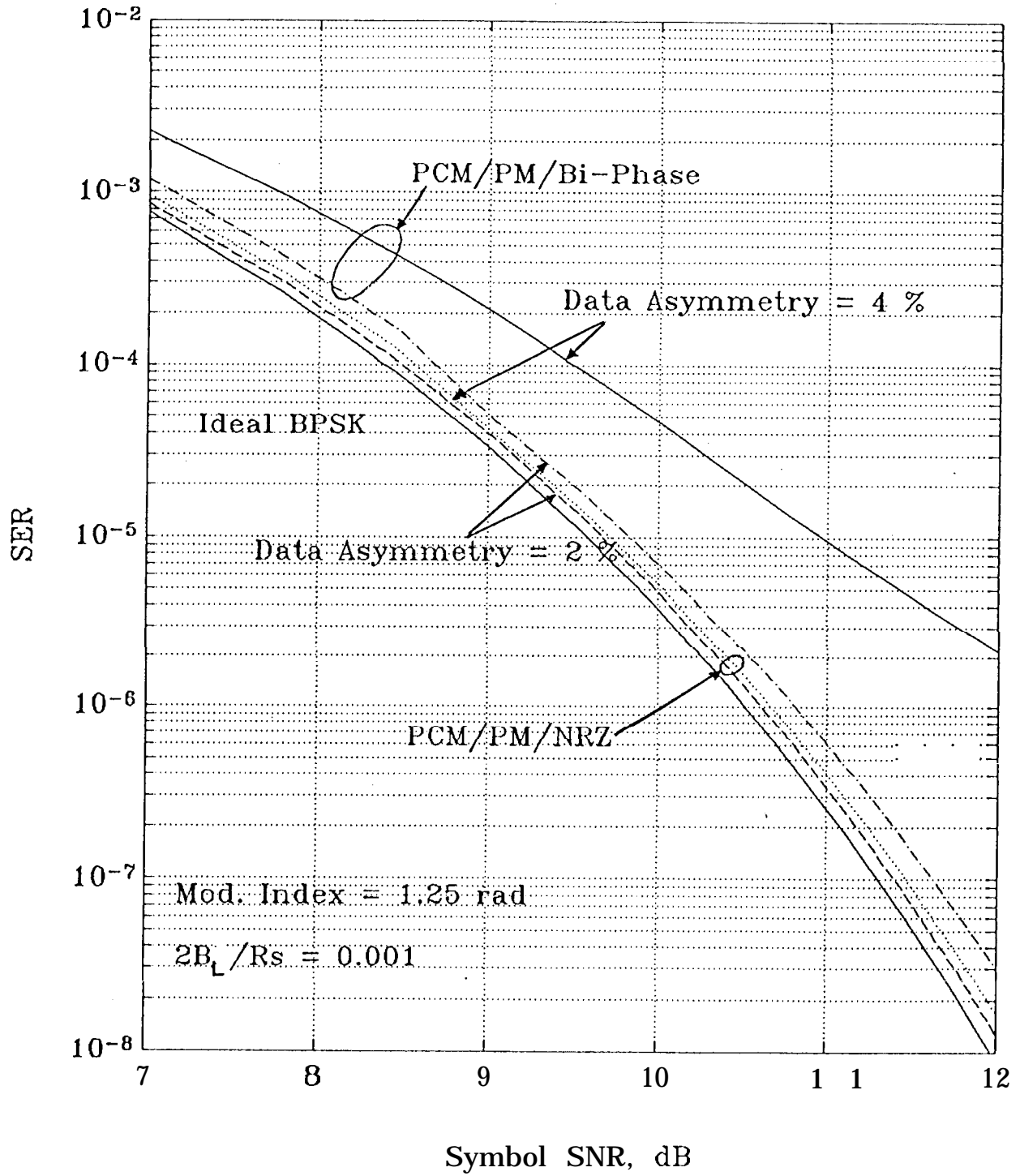


Figure 13. Performance Comparison for Unbalanced Data

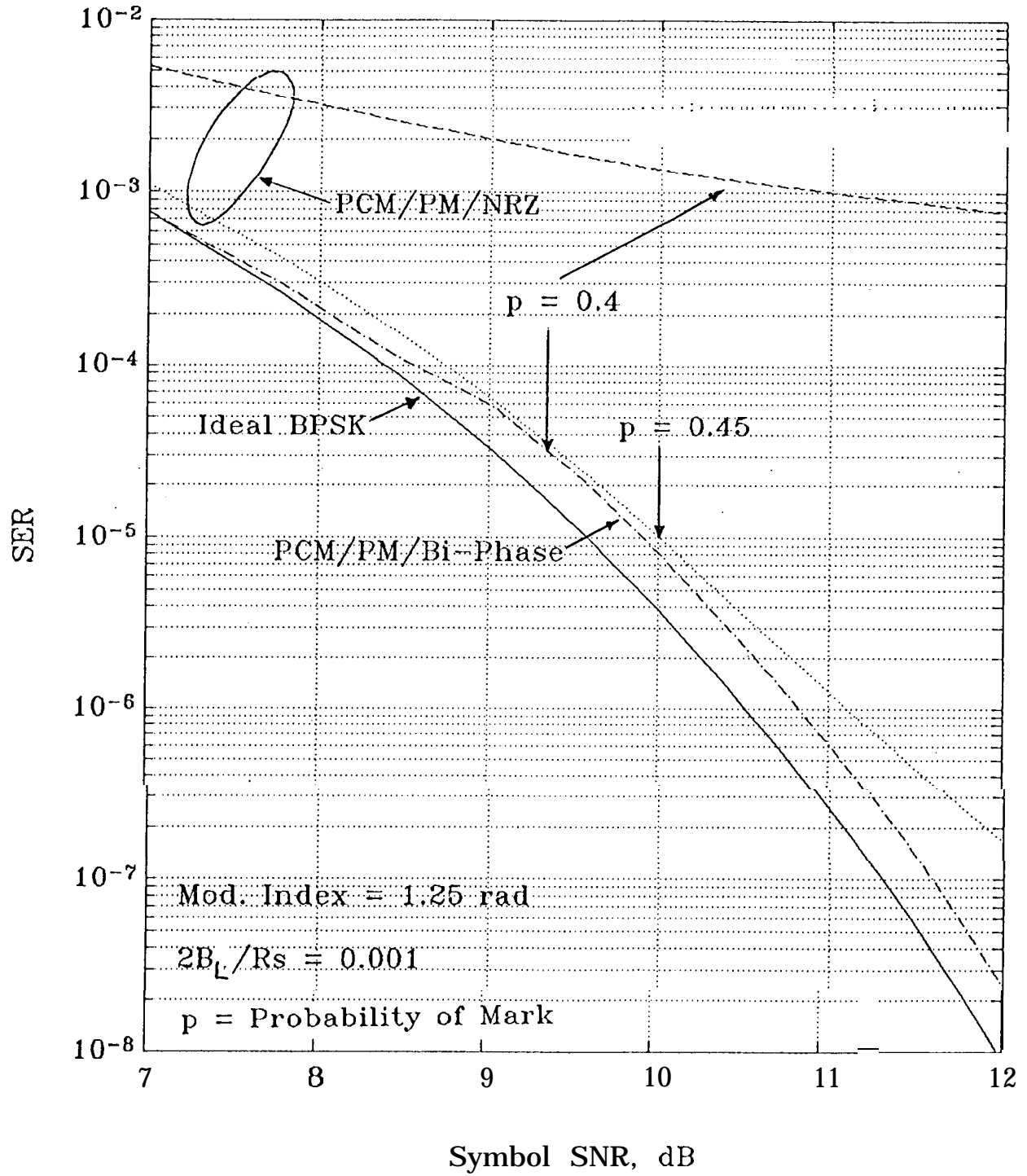


Figure 14. Performance Comparison for 1S1 Channel

